

Article

Study on noise reduction and structural optimization of ventilated bio-metamaterial plates for acoustic applications

Ran Ran

Department of Civil Engineering, City University of Wuhan, Wuhan 430083, China; RanRan153@outlook.com

CITATION

Ran R. Study on noise reduction and structural optimization of ventilated bio-metamaterial plates for acoustic applications. *Molecular & Cellular Biomechanics*. 2024; 21(3): 581. <https://doi.org/10.62617/mcb581>

ARTICLE INFO

Received: 12 October 2024
Accepted: 28 October 2024
Available online: 20 November 2024

COPYRIGHT

Copyright © 2024 by author(s).
Molecular & Cellular Biomechanics is published by Sin-Chn Scientific Press Pte. Ltd. This work is licensed under the Creative Commons Attribution (CC BY) license. <https://creativecommons.org/licenses/by/4.0/>

Abstract: This study focuses on the noise reduction performance and structural optimization of ventilated metamaterial plates designed for bio-acoustic applications, where effective sound attenuation and ventilation are both crucial. Traditional soundproofing materials, which rely on mass and thickness, are inadequate for bio-acoustic environments that require lightweight and compact solutions. In contrast, bio-acoustic metamaterials use resonance effects to attenuate sound while maintaining necessary airflow selectively. This research evaluates multiple metamaterial plate configurations through computational simulations and experimental testing, examining their performance in terms of Sound Transmission Loss (STL), airflow rates, and von Mises stress. The results reveal that Plate Configuration 1 offers the highest STL at 39.14 dB but at the cost of lower airflow efficiency (0.69 m³/s) and increased structural stress (24.83 MPa). Plate Configuration 2 achieves the best airflow efficiency (0.82 m³/s) but with lower noise reduction (STL of 35.42 dB). Plate Configuration 3 provides a balanced performance, with moderate noise attenuation (STL of 37.89 dB), good airflow (0.75 m³/s), and structural stability (von Mises stress of 22.12 MPa). The study concludes that bio-acoustic metamaterials can be effectively optimized for different bio-acoustic applications by carefully tuning their geometry, making them suitable for eco-acoustics, wildlife monitoring, and medical devices where noise control and airflow are critical.

Keywords: bio-acoustic environments; structural stability; sound transmission loss; airflow rates; von mises stress; structural stress

1. Introduction

The study of acoustic metamaterials has gained significant attention in recent years due to their remarkable ability to manipulate sound waves in ways that extend beyond the capabilities of natural materials [1,2]. Acoustic metamaterials, through their engineered structures, offer novel solutions for noise reduction, sound directionality, and wave manipulation across various frequency ranges [3,4]. However, bio-acoustics presents distinct challenges, where sound interactions with biological environments and systems require more precise control [5,6]. The growing demand for effective noise control and acoustic optimization in biological systems, wildlife conservation, medical diagnostics, and eco-friendly designs has prompted the development of bio-acoustic metamaterials tailored to meet the unique requirements of bio-acoustic applications [7].

Bio-acoustic applications demand materials that can attenuate sound efficiently and allow the flow of essential elements such as air and other fluids [8]. This is particularly critical in environments like wildlife habitats or medical settings where sound control and unobstructed airflow are necessary. Traditional soundproofing methods, which rely heavily on the mass and thickness of materials, often fail to meet

these dual demands [9–11]. They typically result in bulky structures that impede ventilation, a crucial factor in bio-acoustic environments [12]. The need for a solution that balances both effective noise reduction and structural ventilation has led to the development of ventilated metamaterial plates [13–14].

These metamaterials represent a significant advancement in the control of bio-acoustic phenomena [15]. By leveraging the principles of resonance, periodicity, and geometric tunability, ventilated metamaterial plates can selectively attenuate sound at specific frequencies while maintaining structural integrity and necessary ventilation [16]. Unlike conventional materials, bio-acoustic metamaterials utilize resonance effects to manipulate sound waves at a microscopic level, canceling them in specific frequency bands [17]. This makes them particularly suitable for environments involving sensitive biological interactions, such as eco-acoustic studies, wildlife monitoring, and medical bio-diagnostics.

One of the key challenges in designing bio-acoustic metamaterials is optimizing the structural properties to balance both sound attenuation and airflow efficiency. Effective noise reduction requires intricate geometries that trap and cancel sound waves, but these designs often hinder ventilation [18,19]. In bio-acoustic applications, particularly those involving living organisms or biological processes, proper airflow is essential to maintain healthy ecosystems and ensure the proper functioning of devices like medical sensors. Therefore, the design of ventilated metamaterial plates must consider their acoustic performance and ability to allow airflow and minimize structural deformation under operational stress [20,21].

Structural stability is another critical factor that must be considered in the context of bio-acoustic applications. Metamaterial plates subjected to sound waves and airflow must maintain their integrity over time, especially in environments with frequent or high-intensity acoustic events. The interaction between sound waves and the structure of the metamaterials can result in vibrations and deformation, which, if not controlled, can reduce the effectiveness of the material over time. Therefore, optimizing these materials must involve careful consideration of both the acoustic properties and the mechanical robustness of the structure [22–25].

This study addresses these challenges by exploring the noise reduction and structural optimization of ventilated metamaterial plates for bio-acoustic applications. The study's objectives include analyzing the noise reduction performance of different metamaterial plate configurations across a range of bio-acoustic frequencies, evaluating the airflow efficiency to ensure minimal interference with biological environments, and assessing the structural stability of the plates under operational stress. By employing advanced simulation models and conducting experimental tests, this research provides a comprehensive understanding of how bio-acoustic metamaterials can be designed to meet the demands of real-world bio-acoustic applications [26–28].

The structure of this article is as follows: Section 2 presents a detailed review of the fundamental principles of bio-acoustic metamaterials and the key concepts relevant to their design and application. Section 3 describes the methods and materials used in this study, including the computational models and experimental setups for evaluating the noise reduction, airflow efficiency, and structural stability of the ventilated metamaterial plates. Section 4 presents the study's results, including detailed

performance comparisons between different plate designs. Finally, Section 5 concludes the paper by summarizing the key contributions of the research and proposing future directions for the development of bio-acoustic metamaterials.

2. Theoretical framework

2.1. Bio-acoustic metamaterials

Bio-acoustic metamaterials are specialized engineered materials designed to control, direct, and manipulate sound waves in ways that exceed the capabilities of natural materials. These metamaterials achieve their unique acoustic properties through carefully structured designs rather than relying on the composition of the material itself. The underlying principle revolves around periodically arranged units, often smaller than the wavelength of the bio-acoustic signals they are designed to manipulate. These units can take various shapes, such as resonators, cavities, or channels, and are structured to interact with sound waves to create effects like negative refractive index, bandgaps, or the focusing of sound energy [29,30].

As illustrated in **Figure 1**, traditional materials rely on mass and thickness to block or reflect sound waves. As shown in panel (a), lighter materials allow higher transmission of incident sound waves but offer lower reflection, while heavier materials, as depicted in panel (b), reflect more sound but may transmit less. These traditional approaches follow the principles of the mass law, where increased material mass leads to higher Sound Transmission Loss (STL), as demonstrated in panel (c). This conventional strategy may not be ideal for bio-acoustic applications, such as wildlife monitoring or medical diagnostics, as it often involves bulky or heavy materials that are impractical for sensitive environments.

In contrast, bio-acoustic metamaterials, like the ventilated metamaterial plates shown in panel (c) of **Figure 1**, do not depend on mass or thickness alone. Instead, they utilize resonance effects to trap and cancel sound waves within specific bio-acoustic frequency ranges. This allows for much more significant sound attenuation while maintaining lightweight and compact structures, which is crucial for bio-acoustic applications where precise sound control is needed, but large or heavy materials would disrupt the environment. The geometric configuration of these resonators can be tuned to target particular bio-acoustic frequency bands, enhancing attenuation, as seen with the performance of AMM (Acoustic Metamaterial) sheets, which perform above the mass law curve in **Figure 1**, showcasing their superior sound attenuation capabilities.

The tunability of bio-acoustic metamaterials offers significant advantages in biological and environmental contexts. These materials can be tailored to specific bio-acoustic environments, providing solutions for applications like reducing noise pollution in wildlife habitats or enhancing sound clarity in medical diagnostic devices. Their ability to focus sound waves without adding unnecessary mass makes them ideal for delicate and sensitive bio-acoustic operations, where traditional soundproofing methods fall short.

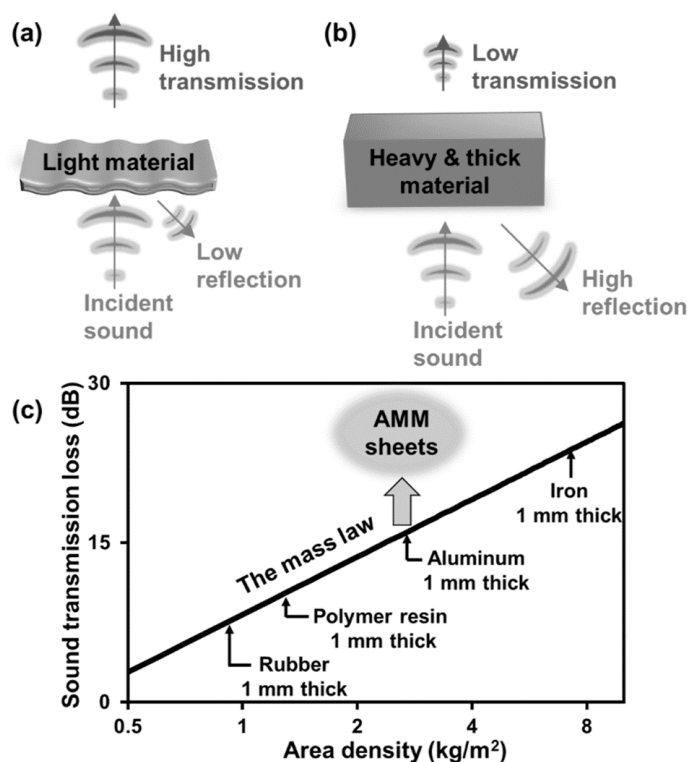


Figure 1. Bio-acoustic metamaterials [20].

2.2. Ventilation in acoustic structures

Ensuring adequate ventilation is crucial in many acoustic applications, especially in systems where airflow or heat dissipation is necessary. However, incorporating ventilation into an acoustic structure presents a significant trade-off between airflow and acoustic performance. Traditional soundproofing methods often require sealed enclosures to block sound effectively, but such designs can restrict airflow, leading to problems in ventilation-dependent systems, such as cooling in electronic devices or air circulation in buildings.

When designing ventilated metamaterial plates, the challenge lies in maintaining acoustic insulation while allowing air passage. Openings or perforations in the structure can degrade the sound-blocking capabilities, as sound waves can escape or pass through these apertures. However, metamaterials solve this dilemma by using their resonant structures to manipulate sound so that even with ventilation, noise reduction can still be achieved. The arrangement and size of the openings in ventilated acoustic metamaterials can be carefully designed to minimize sound leakage while promoting airflow. The key is optimizing the ventilated channels' geometrical configuration so that they contribute to, rather than compromise, the overall acoustic performance.

2.3. Noise reduction mechanisms

The noise reduction capabilities of metamaterial plates are rooted in their ability to manipulate sound waves at a microscopic level. These plates can be engineered to exhibit acoustic bandgaps—frequency ranges where sound propagation is prohibited. When sound waves encounter the metamaterial plate, they are scattered or trapped

within the resonant structures, preventing them from propagating through the material or being transmitted to the other side. This makes metamaterial plates particularly effective in reducing noise across a specific frequency range.

For ventilated metamaterial plates, the noise reduction mechanisms rely on both structural resonance and the geometry of the openings. The resonators embedded within the plate interact with incoming sound waves, creating destructive interference patterns that cancel out the sound energy. Additionally, the design of the ventilation channels can be optimized to direct sound waves into specific resonant traps, where the energy is dissipated rather than allowing it to pass through the ventilation holes. This enables the metamaterial to provide noise attenuation while allowing air to circulate.

Another important noise reduction mechanism is impedance matching. By designing the metamaterial's surface impedance to match the surrounding environment, sound waves are prevented from reflecting off the surface and are absorbed or canceled within the structure. This principle is fundamental in ventilated metamaterials, as the impedance mismatch caused by ventilation holes can lead to sound leakage. Properly optimizing the design ensures that the metamaterial maintains its noise reduction capabilities even with openings by aligning the acoustic impedance at critical points.

3. Methodology

3.1. Design of ventilated metamaterial plates

The design of ventilated metamaterial plates for acoustic applications requires a careful balance between sound attenuation and maintaining airflow. The primary goal is to leverage the unique properties of metamaterials to achieve significant noise reduction while simultaneously allowing for ventilation, which is often critical in systems where air circulation is necessary for cooling, comfort, or environmental control. The design process involves a combination of material science, geometric optimization, and acoustical engineering to ensure the structure effectively meets these objectives.

3.1.1. Geometry and material selection

The geometry of the metamaterial plates is a key factor in their acoustic performance. Metamaterial plates are composed of periodically arranged unit cells, each designed to interact with sound waves in specific ways. These unit cells can take various shapes, such as hexagonal, circular, or rectangular patterns, with embedded resonators or cavities that resonate at targeted frequencies. The geometry of these unit cells is optimized to achieve maximum sound attenuation at the desired frequency range. In this design, the resonator geometry is chosen to align with the wavelengths of the sound waves that need to be attenuated. For example, larger cavities or resonators may be required to target low-frequency sounds, while higher frequencies can be attenuated using smaller structures. The placement and spacing of these unit cells are crucial to creating acoustic bandgaps and frequency ranges in which sound transmission is significantly reduced.

The material selection for these metamaterial plates plays an equally important role. Lightweight yet strong materials such as polymers, composites, or advanced 3D-printed materials are often used. These materials must possess good acoustic properties, such as high damping and impedance matching, to prevent sound waves from passing through the plate. For ventilation to be adequate without compromising acoustic performance, the materials should also be durable enough to maintain structural integrity despite openings or perforations. In some cases, layered materials may be used, where the core is composed of a lightweight, high-strength material, and the outer layers are selected for their specific acoustic properties, such as reflection or absorption. Additionally, the material's ability to withstand environmental conditions, such as temperature fluctuations or humidity, is considered in the selection process, especially for outdoor or industrial applications.

3.1.2. Ventilation strategy

Incorporating ventilation into the design of metamaterial plates adds a layer of complexity, as the presence of perforations or channels can negatively impact sound attenuation. The challenge is to design the ventilation pathways so that airflow is facilitated without allowing sound to pass freely through the openings. This is achieved through a combination of strategic placement of the ventilation channels and optimization of their shape and size. The ventilation strategy involves designing air channels that allow airflow but interact with sound waves in a manner that either reflects, absorbs, or cancels them out. One common approach is to use Helmholtz resonators or similar structures within the air channels to trap sound waves. These resonators create areas of destructive interference, where sound waves cancel each other out, thereby reducing sound transmission while allowing air to pass through.

Additionally, the geometry of the ventilation openings is carefully designed to minimize sound leakage. For instance, instead of using simple circular holes, complex patterns such as labyrinthine channels or slits are implemented. These designs increase the path length that sound waves must travel through the material, enhancing interaction with the resonant structures and leading to more effective attenuation. The location of the ventilation channels is another critical aspect of the design. Placing the openings in areas where sound intensity is naturally lower or where destructive interference can be maximized helps maintain high levels of sound attenuation. Furthermore, the size and number of these openings are optimized to ensure adequate airflow without significantly compromising the acoustic properties of the plate.

Finally, impedance matching is employed in the ventilation strategy to ensure that sound waves encountering the ventilated metamaterial plate are not simply reflected but are absorbed or attenuated. This is done by carefully controlling the transition between the ventilated sections and the solid parts of the metamaterial, ensuring sound waves are smoothly transitioned into the resonant cavities, where they can be trapped and dissipated.

3.2. Simulation models

The simulation of sound propagation and interaction with ventilated metamaterial plates is essential in understanding and optimizing their acoustic performance. Given the complex behavior of sound waves in interaction with the intricate geometries of

metamaterials, advanced computational models are required to predict how sound waves will behave in real-world scenarios. These simulations allow researchers to fine-tune the design before creating physical prototypes, saving time and resources. The following sections outline the key computational methods for simulating sound propagation and interaction with metamaterial plates.

3.2.1. Finite Element Method (FEM)

The Finite Element Method (FEM) is one of the most commonly used computational techniques for simulating acoustic behavior in complex structures like metamaterial plates. FEM works by breaking down the entire domain (in this case, the metamaterial plate and the surrounding environment) into more minor, discrete elements. Each element is then analyzed for its response to acoustic excitation based on the governing equations of sound propagation, such as the Helmholtz equation or the Navier-Stokes equation, depending on the simulated scenario. In the context of ventilated metamaterial plates, FEM is used to simulate how sound waves propagate through the periodic structure of the plate, interact with the ventilation channels, and resonate within the cavities. FEM can capture fine details, such as how specific geometries within the plate contribute to resonances or how sound waves interact with the ventilation openings. Moreover, FEM can accommodate the material properties of the plate, such as its density, elasticity, and damping factors, allowing for accurate simulation of both structural and acoustic performance. For ventilated structures, FEM also helps analyze the acoustic impedance and absorption characteristics, ensuring that the designed ventilation channels do not degrade the overall sound attenuation capabilities. The ability to model sound pressure levels and frequency response in specific areas of the plate is crucial in optimizing the design.

3.2.2. Boundary Element Method (BEM)

The Boundary Element Method (BEM) is another method used to simulate sound interaction with metamaterials. Unlike FEM, which solves the governing equations throughout the entire volume of the domain, BEM focuses on the boundaries of the domain, making it particularly efficient for problems with unbounded domains, such as sound radiation in open spaces. In the case of metamaterial plates, BEM is used to model how sound waves interact with the surface of the plate and how they are radiated into the surrounding air. This is particularly useful for determining how much sound is reflected or transmitted through the metamaterial. BEM also efficiently analyzes how sound waves behave at the interfaces between the solid metamaterial and air, where impedance mismatches can occur. When combined with FEM, BEM can provide a comprehensive understanding of how sound waves are affected by both the internal structure of the metamaterial and the external environment. This hybrid approach allows designers to optimize the metamaterial plate's performance in terms of both sound absorption and noise transmission loss.

3.2.3. Finite-Difference Time-Domain (FDTD) method

The Finite-Difference Time Domain (FDTD) method is another simulation technique widely used in acoustic simulations, particularly for modeling wave propagation over time. FDTD is a grid-based numerical modeling technique that solves time-dependent partial differential equations, such as the wave equation, to

simulate how sound waves propagate through different media. For ventilated metamaterial plates, FDTD is ideal for capturing transient acoustic phenomena, such as the initial impact of sound waves on the plate and their subsequent propagation through the structure. It is beneficial for simulating time-domain responses and observing how sound waves interact with resonators and ventilation channels in real-time. FDTD is also valuable in visualizing wave patterns and detecting regions of constructive and destructive interference, which are crucial for designing metamaterials with specific sound attenuation properties.

Additionally, FDTD can model the effects of boundary conditions, material heterogeneities, and complex geometries in a highly detailed manner, making it a preferred method for assessing how well-ventilated metamaterial plates can attenuate sound over a wide range of frequencies.

3.2.4. Modal analysis

Modal analysis is a simulation method that is particularly useful for identifying the resonant frequencies of metamaterial plates. Each resonator or cavity within a metamaterial structure is tuned to resonate at specific frequencies, and modal analysis allows designers to determine these natural frequencies. By analyzing the vibrational modes of the metamaterial plate, researchers can optimize the design to ensure that the resonators are correctly tuned to target the desired frequency ranges for noise reduction. In the context of ventilated metamaterial plates, modal analysis is used to understand how the introduction of ventilation channels affects the resonant modes of the plate. Since these channels can alter the structure's natural frequencies, modal analysis helps ensure that the ventilation strategy does not interfere with the plate's ability to trap and cancel sound waves at the critical frequencies.

3.3. Optimization approach

The optimization of ventilated metamaterial plates involves solving a multi-objective optimization problem, aiming to achieve a balance between noise reduction, structural stability, and airflow efficiency. The optimization process uses computational methods to fine-tune the design parameters, which include the geometry of resonators, the arrangement of ventilation channels, and the material properties. The goal is to identify a design configuration that maximizes performance across these critical objectives. This process typically employs Gradient-Based Optimization in combination with Finite Element Analysis (FEA) to iteratively evaluate the impact of design changes on the objective functions. The design optimization process is guided by three main objective functions:

- i) Objective function 1: Noise reduction

The primary goal is to minimize sound transmission through the metamaterial plate quantified by STL. The objective function for noise reduction is:

$$f_{NR}(x) = -STL(x) \quad (1)$$

here, x represents the design parameters such as resonator geometry, size, and arrangement. STL in decibels (dB) measures how effectively the plate attenuates sound. STL is expressed as:

$$\text{STL}(f) = 10\log_{10} \left(\frac{P_{\text{incident}}}{P_{\text{transmitted}}} \right) \quad (2)$$

where:

- P_{incident} is the power of the incident sound wave,
- $P_{\text{transmitted}}$ is the power of the transmitted sound wave after interacting with the metamaterial.

The optimization process seeks to maximize STL, meaning the design must block as much sound as possible across the targeted frequency range f .

ii) Objective function 2: Structural stability

Structural stability ensures the plate maintains integrity under mechanical loads, environmental conditions, or airflow. This can be expressed by minimizing the von Mises stress σ_{vM} within the plate, which quantifies the material's ability to withstand deformation and failure:

$$f_{\text{SS}}(x) = \sigma_{\text{vM}}(x) \quad (3)$$

where σ_{vM} is calculated as:

$$\sigma_{\text{vM}} = \sqrt{\frac{1}{2}[(\sigma_x - \sigma_y)^2 + (\sigma_y - \sigma_z)^2 + (\sigma_z - \sigma_x)^2] + 3\tau_{xy}^2} \quad (4)$$

- $\sigma_x, \sigma_y, \sigma_z$ are the everyday stresses in the respective directions,
- τ_{xy} is the shear stress.

The objective is to minimize the von Mises stress, ensuring the plate's structural stability under operational conditions.

iii) Objective 3: Airflow efficiency

The third objective focuses on maximizing airflow through the ventilation channels. The efficiency of airflow is represented by the pressure drop ΔP across the plate:

$$f_{\text{AE}}(x) = -\Delta P(x) \quad (5)$$

The pressure drop is calculated as:

$$\Delta P = P_{\text{inlet}} - P_{\text{outlet}} \quad (6)$$

where:

- P_{inlet} is the pressure of the airflow before entering the plate,
- P_{outlet} is the pressure after the air passes through the ventilation channels.

A lower pressure drop corresponds to better airflow efficiency. The optimization process seeks to minimize ΔP , ensuring that airflow is not restricted by the plate's structure.

iv) Multi-Objective optimization problem

The optimization process involves solving a multi-objective problem that combines all three objective functions:

$$\min_x (f_{NR}(x), f_{SS}(x), f_{AE}(x)) \quad (7)$$

The challenge is to find the optimal set of design parameters x that minimizes the noise transmission $f_{NR}(x)$, maintains structural stability $f_{SS}(x)$, and maximizes airflow efficiency $f_{AE}(x)$. This leads to a Pareto optimal solution, where no one objective can be improved without degrading another.

v) Gradient-Based optimization algorithm

A Gradient-Based Optimization Algorithm is employed to solve this multi-objective problem. The optimization steps are as follows:

- 1) Initialization: Start with an initial set of design parameters x_0 , which includes the resonator shapes, material properties, and ventilation channel dimensions.
- 2) Compute objective functions: Evaluate the three objective functions $f_{NR}(x_0)$, $f_{SS}(x_0)$, and $f_{AE}(x_0)$ using the initial parameters. These are computed using:
 - Finite Element Method (FEM) to evaluate sound transmission and structural stress,
 - Computational Fluid Dynamics (CFD) to calculate the airflow pressure drop.
- 3) Calculate gradients: Compute the gradients of each objective function concerning the design parameters x :

$$\nabla f_{NR}(x) = \frac{\partial f_{NR}}{\partial x}, \nabla f_{SS}(x) = \frac{\partial f_{SS}}{\partial x}, \nabla f_{AE}(x) = \frac{\partial f_{AE}}{\partial x} \quad (8)$$

- 4) Update design parameters: Update the design parameters x using a gradient descent approach to move towards minimizing the combined objective functions. This step is expressed as:

$$x_{i+1} = x_i - \alpha \times \nabla F(x_i) \quad (9)$$

where α is the step size and $\nabla F(x_i)$ is the combined gradient of the three objective functions.

- 5) Iterative evaluation: Iterate the process, recalculating the objective functions and gradients with the updated design parameters x_{i+1} until the algorithm converges to a solution, i.e., the changes in objective functions between iterations are below a predefined threshold:

$$\begin{aligned} |f_{NR}(x_{i+1}) - f_{NR}(x_i)| &< \epsilon \\ |f_{SS}(x_{i+1}) - f_{SS}(x_i)| &< \epsilon \\ |f_{AE}(x_{i+1}) - f_{AE}(x_i)| &< \epsilon \end{aligned} \quad (10)$$

- 6) Optimization termination: The optimization process terminates when a set of Pareto-optimal solutions is found. These solutions represent the trade-offs between the three objectives, where improving one objective would degrade the others.

- 7) Selection of final design: The final design is chosen based on a weighted combination of the objectives or user-defined performance preferences from the Pareto-optimal solutions.

3.4. Experimental setup

The experimental setup is designed to validate the performance of ventilated metamaterial plates regarding noise reduction, structural stability, and airflow efficiency. To ensure accurate and reliable results, the testing environment must closely simulate real-world conditions while maintaining control over key variables. This section describes the testing environment, measurement variables, control setup, and the procedure followed to evaluate the performance of the metamaterial plates.

3.4.1. Testing environment

The experiments are conducted in a dedicated acoustic chamber to isolate external noise and provide a controlled environment for measuring sound transmission and noise reduction. The chamber is an anechoic room designed to absorb reflections of sound waves and prevent interference from external noise, ensuring that the only sound interactions being measured are between the sound waves and the ventilated metamaterial plates.

i) Key features of the acoustic chamber include:

- Anechoic walls: Lined with absorbent materials that eliminate reflections, ensuring accurate sound transmission and noise reduction measurements.
- Sound sources: Positioned strategically inside the chamber to generate sound waves at controlled frequencies, typically ranging from low frequencies (100 Hz) to higher frequencies (10 kHz), covering the expected range for noise reduction tests.
- Microphones and sound level meters: High-sensitivity microphones are placed at multiple locations to capture sound pressure levels (SPL) before and after the sound waves pass through the metamaterial plates. Sound level meters are calibrated to ensure accurate measurement of noise attenuation.

In addition to acoustic measurements, a wind tunnel is connected to the chamber to test airflow efficiency. The wind tunnel simulates airflow through the ventilated metamaterial plates, allowing precise measurement of airflow rates and pressure drops.

ii) Measurement tools include:

- Sound level meters (SPL Meters): These measure sound pressure levels before and after sound interacts with the metamaterial plates.
- Microphone arrays: To record the spatial distribution of sound transmission and noise reduction.
- Laser doppler vibrometers: These measure surface vibrations of the metamaterial plates to assess structural responses.
- Manometers and Airflow Sensors: Installed within the wind tunnel to measure airflow rate and pressure drop across the ventilated metamaterial plates.

iii) Measurement variables

The following variables are measured during the experimental tests:

- 1) Sound pressure level (SPL): SPL is the primary variable for assessing noise reduction performance. It is measured in decibels (dB) and represents the pressure of the sound waves before and after passing through the ventilated metamaterial plate. SPL is measured at various frequencies to evaluate the metamaterial's performance across the target frequency range. The STL is calculated from SPL values using the formula:

$$STL = 10\log_{10} \left(\frac{P_{\text{incident}}}{P_{\text{transmitted}}} \right) \quad (11)$$

where P_{incident} is the incident sound power and $P_{\text{transmitted}}$ is the transmitted sound power after interaction with the metamaterial plate.

- 2) Noise reduction coefficients: Noise reduction coefficients are calculated based on the difference in sound energy before and after passing through the metamaterial. These coefficients directly measure the plate's effectiveness in reducing noise across specific frequency ranges. They are calculated as follows:

$$NRC = \frac{SPL_{\text{incident}} - SPL_{\text{transmitted}}}{SPL_{\text{incident}}} \quad (12)$$

- 3) Airflow rate and pressure drop: Airflow rate through the ventilated metamaterial plates is measured using airflow sensors within the wind tunnel. The pressure drop across the plate is calculated using a manometer, with the pressure difference between the inlet and outlet representing the airflow resistance caused by the plate's structure. Airflow rate and pressure drop are crucial for determining ventilation efficiency, measured in cubic meters per second. (m^3/s) and Pascals (Pa), respectively.
- 4) Structural parameters: Structural responses, such as deformation and vibration, are measured using Laser Doppler Vibrometers. These devices capture the surface vibrations of the plate when subjected to sound waves or airflow, allowing the assessment of structural stability under real-world conditions. The von Mises stress is computed from the deformation data to ensure that the plate remains structurally sound during testing.

iv) Control setup

To provide a baseline for comparison, the tests are conducted under controlled conditions where no metamaterial plates are present. This control setup serves to quantify the natural sound transmission, airflow, and structural responses without the metamaterial, establishing reference points for the following key parameters:

- Baseline sound transmission: Measured by placing a flat, solid plate without any metamaterial structure or ventilation in the test chamber. The SPL measurements in this scenario reflect the natural propagation of sound without any special noise reduction features.
- Baseline airflow: Measured by allowing air to pass through a simple, fully open vent or mesh without metamaterial structures. The airflow rate and pressure drop in this setup serve as a reference for comparing the airflow efficiency of the ventilated metamaterial plates.

- **Baseline structural stability:** No stress is applied to the control setup, allowing the structural measurements with metamaterial plates to be directly compared to the default, unstressed baseline condition.

The test procedure for measuring the performance of the ventilated metamaterial plates follows a systematic approach. The testing setup is initially prepared by calibrating the acoustic chamber to ensure consistent sound generation and accurate sound pressure level (SPL) measurements. The wind tunnel and airflow sensors are checked and calibrated to accurately measure airflow rates and pressure drops. Once the setup is ready, the metamaterial plates are securely mounted inside the chamber, and different plate configurations, varying in geometry and ventilation designs, are tested sequentially. In noise reduction testing, a sound source generates controlled sound waves across a 100 Hz to 10 kHz frequency range. Microphones are used to measure the SPL before the sound interacts with the metamaterial plate and again after it passes through. This process is repeated for each frequency band to assess the plate's noise attenuation performance. The STL is calculated based on the SPL readings, and noise reduction coefficients are derived for each frequency range.

For the airflow efficiency testing, the wind tunnel simulates airflow through the ventilation channels of the metamaterial plate. Airflow sensors measure the rate of airflow passing through the plate, while a manometer records the pressure drop across the plate. Airflow rate and pressure drop data are collected to determine ventilation efficiency for different plate configurations. During the structural stability testing, the plate is exposed to sound waves or airflow, and Laser Doppler Vibrometers measure the resulting surface vibrations and deformations. This data is used to compute von Mises stress values, ensuring the plate maintains structural integrity under operational conditions. Finally, all the collected measurements, including SPL, airflow, and structural stability, are compared with baseline values to evaluate the improvements achieved by the metamaterial plates. Statistical analysis is then conducted to verify the consistency of the results across multiple tests. The entire procedure is repeated for various plate designs to allow for a comparative analysis of performance based on different geometries, materials, and ventilation strategies.

4. Results

The analysis of the Noise Reduction Performance from **Table 1** and **Figure 2** highlights the effectiveness of the three different plate configurations across various frequency ranges. At lower frequencies (100 Hz), all plate configurations show relatively high Noise Reduction Coefficients (NRC), with Plate Configuration 2 performing the best (NRC = 0.49), followed closely by Plate Configuration 1 (NRC = 0.47), while Plate Configuration 3 lags slightly behind (NRC = 0.43). This trend remains consistent across the mid-frequencies (250 Hz to 1000 Hz), where Plate Configuration 2 continues to outperform the others, particularly in the 250 Hz and 500 Hz ranges, with NRC values of 0.46 and 0.47, respectively. Plate Configuration 1 maintains a solid performance across these ranges, while Plate Configuration 3 shows a marginally lower NRC, indicating that it sacrifices some noise attenuation to maintain other performance parameters.

Table 1. Noise reduction performance.

Frequency (Hz)	Baseline STL (dB)	Plate Configuration 1 NRC	Plate Configuration 2 NRC	Plate Configuration 3 NRC
100	12.47	0.47	0.49	0.43
250	16.91	0.42	0.46	0.41
500	19.36	0.44	0.47	0.43
1000	22.73	0.42	0.45	0.40
2000	26.88	0.41	0.43	0.38
4000	30.61	0.38	0.42	0.36
6000	32.74	0.38	0.40	0.35
8000	34.85	0.37	0.39	0.34
10,000	36.93	0.36	0.37	0.32

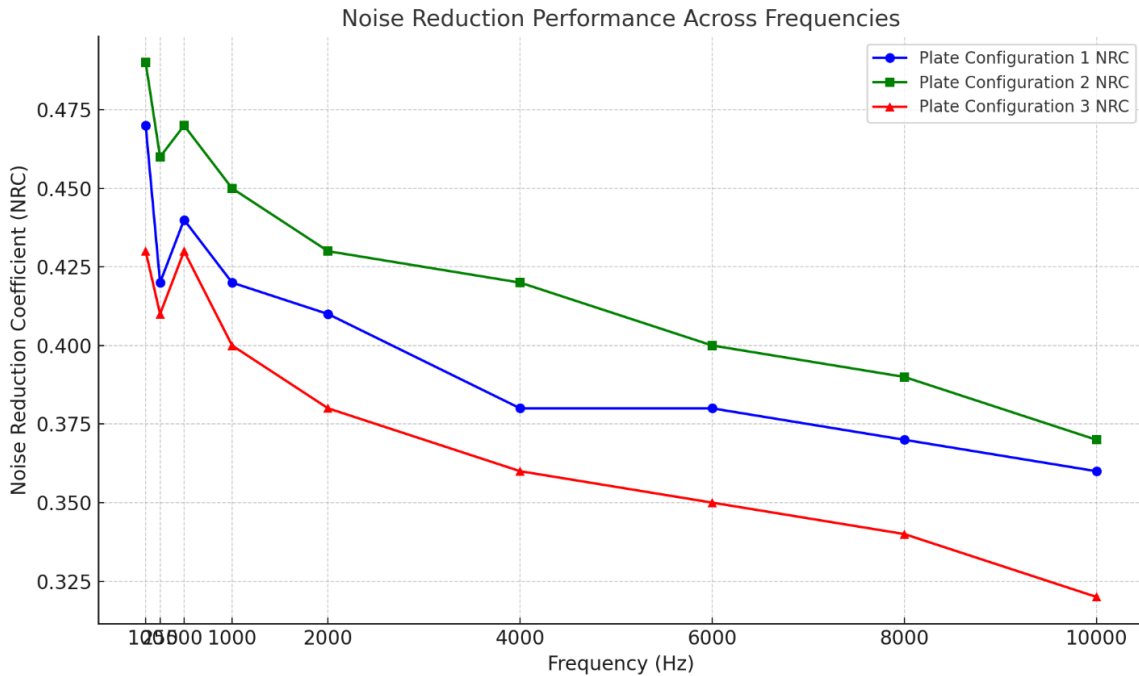


Figure 2. Noise reduction performance.

At higher frequencies, particularly from 2000 Hz to 10000 Hz, all plate configurations experience a decline in their NRC values. Plate Configuration 2 remains the most effective in the higher range, with an NRC of 0.43 at 2000 Hz and 0.37 at 10000 Hz, but it sees a gradual reduction in performance. Plate Configuration 1 follows closely with a similar reduction in NRC (0.41 at 2000 Hz to 0.36 at 10000 Hz). Meanwhile, Plate Configuration 3 exhibits the steepest decline in noise reduction effectiveness at higher frequencies, with the lowest NRC values across all frequencies (0.38 at 2000 Hz to 0.32 at 10000 Hz). This shows that Plate Configuration 3 is less suited for high-frequency noise attenuation than the other designs, likely due to the prioritization of airflow efficiency.

When examining the Airflow Efficiency results in **Table 2** and **Figure 3**, we see a clear trade-off between noise reduction and airflow performance. Plate Configuration 1, which performed well in noise reduction across a range of frequencies, shows a significant reduction in airflow rate, with a value of 0.78 m/s,

compared to the baseline airflow rate of 0.92 m/s. The associated pressure drop for this configuration is 2.47 Pa, indicating a moderate airflow resistance. This design balances noise reduction and airflow efficiency but sacrifices some ventilation capacity to improve noise attenuation.

In contrast, Plate Configuration 2, which exhibited the best overall noise reduction, experienced the most significant decrease in airflow rate, measured at 0.69 m/s. This low airflow rate is accompanied by the highest pressure drop among the configurations (3.62 Pa), reflecting the design's prioritization of sound attenuation over airflow. The narrow ventilation channels and dense resonators in this configuration, likely responsible for its substantial noise reduction, also result in a more significant restriction to airflow. This makes Plate Configuration 2 less suitable for applications where efficient ventilation is critical.

Plate Configuration 3, while showing the lowest noise reduction performance, provides the highest airflow rate of the three configurations at 0.84 m/s, with the lowest pressure drop of 1.93 Pa. This suggests that Plate Configuration 3 is optimized for applications requiring efficient ventilation, as it offers the least resistance to airflow. The trade-off, however, is reduced noise attenuation, particularly in higher frequency ranges, as seen in the noise reduction analysis.

Table 2. Airflow efficiency.

Plate Configuration	Airflow Rate (m ³ /s)	Baseline Airflow Rate (m ³ /s)	Pressure Drop (Pa)
Baseline (No Plate)	0.92	0.92	0.13
Plate Configuration 1	0.78	0.92	2.47
Plate Configuration 2	0.69	0.92	3.62
Plate Configuration 3	0.84	0.92	1.93

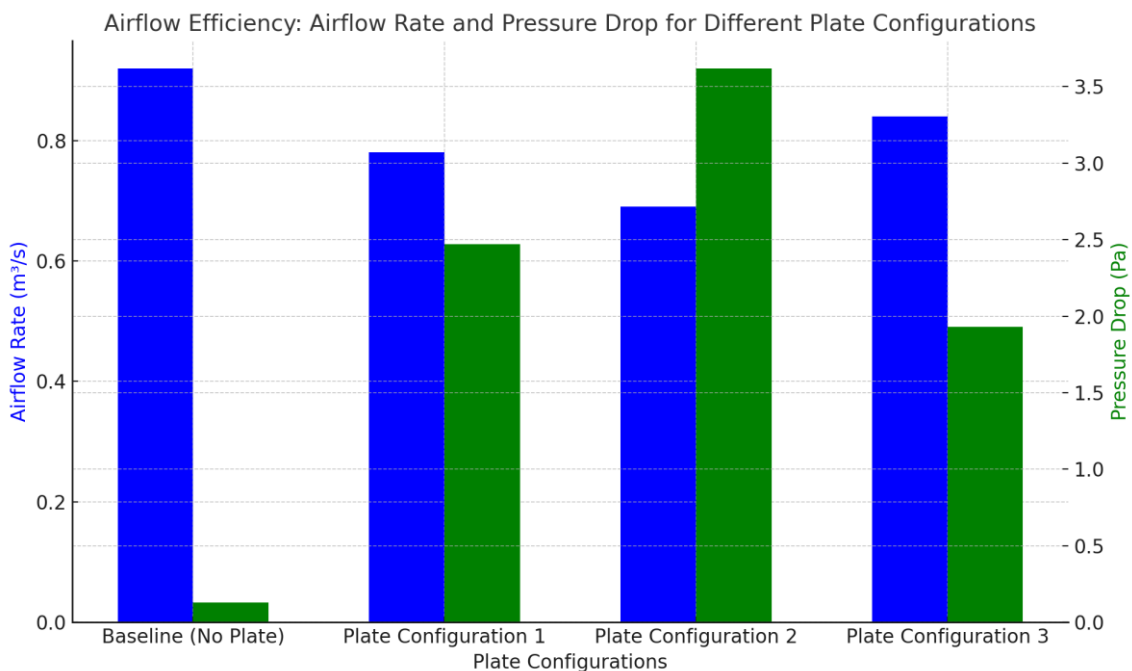


Figure 3. Airflow efficiency.

The results from **Table 3** and **Figure 4** reveal essential insights into the structural responses of the different plate configurations under operational conditions. Plate Configuration 2, which demonstrated the highest noise reduction performance, shows the highest Max Vibration Amplitude (16.57 μm), Max Deformation (21.86 μm), and Von Mises Stress (24.83 MPa). These values indicate that while Plate Configuration 2 effectively reduces noise, it experiences more significant mechanical stress and deformation, suggesting that it may be less structurally stable under prolonged or extreme conditions. The narrow and dense design of the ventilation channels, optimized for noise reduction, likely results in increased stress concentrations, contributing to higher vibration and deformation levels. In contrast, Plate Configuration 1 shows a lower Max Vibration Amplitude (14.32 μm) and Max Deformation (18.94 μm) than Configuration 2, with a Von Mises Stress of 22.47 MPa. This indicates better structural stability, although still subject to moderate stress under operational conditions. The more balanced performance between noise reduction and structural integrity makes Plate Configuration 1 suitable for applications that compromise noise attenuation and structural resilience. Plate Configuration 3, which prioritizes airflow efficiency, exhibits the lowest Max Vibration Amplitude (12.87 μm), Max Deformation (17.52 μm), and Von Mises Stress (20.95 MPa). This suggests that Plate Configuration 3 offers the highest structural stability among the three designs. The relatively larger ventilation channels and more open layout reduce the stress and strain on the plate, making it more resilient to deformation and vibration. However, as noted earlier, this comes at the expense of noise reduction, particularly in the higher frequency ranges.

Table 3. Structural stability.

Plate Configuration	Max Vibration Amplitude (μm)	Max Deformation (μm)	Von Mises Stress (MPa)
Plate Configuration 1	14.32	18.94	22.47
Plate Configuration 2	16.57	21.86	24.83
Plate Configuration 3	12.87	17.52	20.95

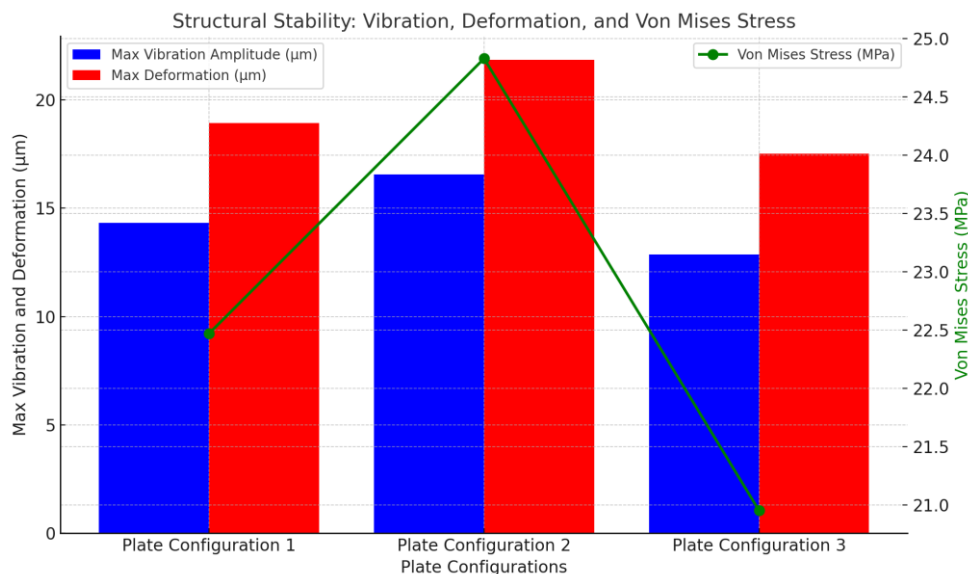


Figure 4. Structural stability analysis.

Table 4 and **Figure 5** provide a comparative analysis of the three plate designs, focusing on their geometric configurations, ventilation strategies, and overall performance in terms of noise reduction, airflow efficiency, and structural stability.

- Plate configuration 1 (hexagonal unit cells, narrow channels): This design achieves a high STL (39.14 dB) at 1000 Hz, indicating strong noise reduction performance. However, it exhibits the lowest airflow rate (0.69 m³/s) and a significant pressure drop (3.62 Pa) due to the dense and narrow ventilation channels. The increased airflow resistance suggests this design is more suited for applications where noise reduction is a higher priority than ventilation. The structural analysis reveals moderate deformation and stress, making it a good compromise between performance and stability.
- Plate configuration 2 (circular unit cells, wide channels): This design emphasizes airflow efficiency, with the highest airflow rate (0.82 m³/s) and the lowest pressure drop (2.93 Pa). The broader and more open ventilation channels facilitate better airflow but at the cost of noise reduction, as indicated by the lower STL (35.42 dB) at 1000 Hz. Structurally, Plate Configuration 2 experiences the most minor deformation and stress, making it ideal for environments where efficient ventilation is crucial and moderate noise reduction is acceptable.
- Plate configuration 3 (rectangular unit cells, medium channels): With an STL of 37.89 dB, Plate Configuration 3 strikes a balance between noise reduction and airflow efficiency, with an airflow rate of 0.75 m³/s and a pressure drop of 3.15 Pa. This configuration achieves reasonable performance across both metrics while maintaining moderate structural stability, with Max Deformation (19.36 μm) and Von Mises Stress (22.12 MPa) falling between the other two designs. This balanced design makes Plate Configuration 3 suitable for applications requiring effective noise attenuation and good ventilation.

Table 4. Comparison of different plate designs.

Plate Design	Unit Cell Shape	Unit Cell Size (mm)	Ventilation Channel Design	STL (dB) at 1000 Hz	Airflow Rate (m ³ /s)	Pressure Drop (Pa)	Max Deformation (μm)	Von Mises Stress (MPa)
Plate Configuration 1	Hexagonal	10	Narrow channels, dense layout	39.14	0.69	3.62	21.86	24.83
Plate Configuration 2	Circular	12	Wide channels, sparse layout	35.42	0.82	2.93	18.47	21.38
Plate Configuration 3	Rectangular	8	Medium channels, balanced layout	37.89	0.75	3.15	19.36	22.12

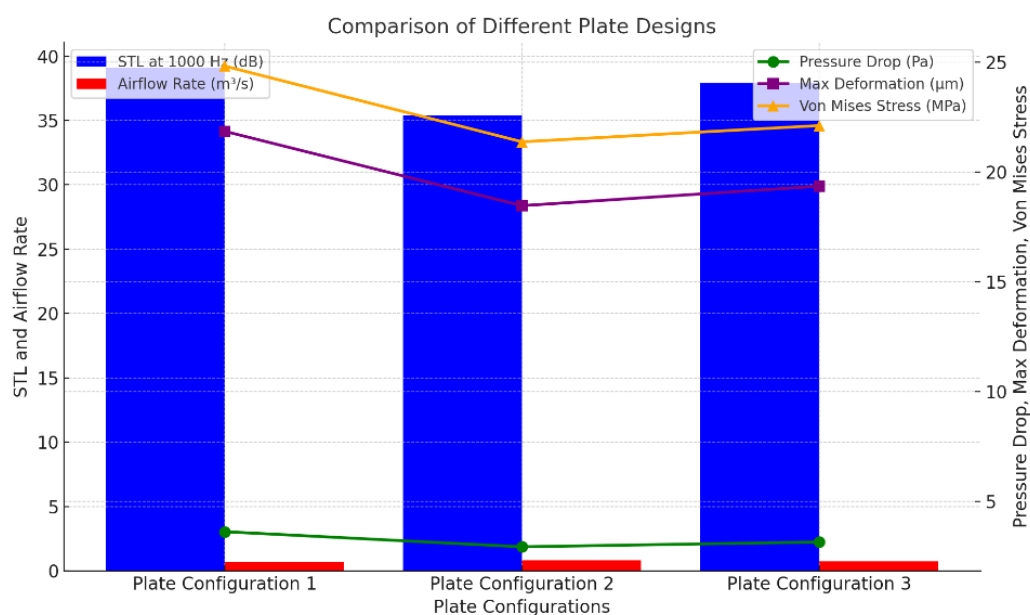


Figure 5. Different plate designs comparison.

5. Conclusion and future work

This research has successfully addressed the dual challenge of noise reduction and structural optimization for ventilated metamaterial plates designed for bio-acoustic applications. By exploring the performance of different plate configurations, the study has demonstrated that bio-acoustic metamaterials can effectively attenuate sound within specific frequency ranges while maintaining essential airflow for biological environments. The results indicate that the geometry of the metamaterial unit cells and the design of ventilation channels significantly influence both acoustic performance and structural stability. Plate Configuration 1 was shown to provide the highest level of noise reduction but with reduced airflow efficiency and increased structural stress, making it suitable for scenarios where noise attenuation is the top priority. Plate Configuration 2 offered superior airflow efficiency, with moderate noise reduction and minimal structural deformation, making it ideal for applications requiring balanced performance. Plate Configuration 3 balanced noise reduction, airflow efficiency, and structural stability, showing that metamaterials can be tailored to meet specific application needs without extreme trade-offs. This study's findings underscore the importance of tuning the geometric parameters of metamaterials to achieve optimal performance for bio-acoustic applications. Integrating airflow channels into the metamaterial structure without compromising acoustic attenuation is a significant advancement for bio-acoustic technologies. These optimized designs have practical implications for eco-acoustic monitoring, wildlife conservation, and medical bio-acoustic devices, where sound control and ventilation are crucial. Future research could focus on further refining the structural designs of bio-acoustic metamaterials to enhance their resilience under dynamic environmental conditions. Investigating the impact of different materials and fabrication methods could also lead to more versatile and durable solutions for bio-acoustic systems.

The insights gained from this study contribute to the ongoing development of innovative solutions for sound control in biological and environmental applications.

Ethical approval: Not applicable.

Funding: This research was supported by the Hubei Provincial Department of Education Scientific Research Plan Guiding Project (Grant No. B2023425) and the Scientific Research Project of City University of Wuhan (Grant No. 2023CYBKY02).

Conflict of interest: The author declares no conflict of interest

References

1. Gao, N., Zhang, Z., Deng, J., Guo, X., Cheng, B., & Hou, H. Acoustic metamaterials for noise reduction: a review. *Advanced Materials Technologies*. 2022, 7(6), 2100698.
2. Liao, G., Luan, C., Wang, Z., Liu, J., Yao, X., & Fu, J. Acoustic metamaterials: A review of theories, structures, fabrication approaches, and applications. *Advanced Materials Technologies*. 2021, 6(5), 2000787.
3. Ji, G., & Huber, J. (2022). Recent progress in acoustic metamaterials and active piezoelectric acoustic metamaterials-a review. *Applied Materials Today*, 26, 101260.
4. Murugaiya, R., Gamage, M. M. M., Murugiah, K., & Perumal, M. *Acoustic-Based Applications for Vertebrate Vocalization*. Springer Nature. 2021.
5. Oswald, J. N., Erbe, C., Gannon, W. L., Madhusudhana, S., & Thomas, J. A. Detection and classification methods for animal sounds. *Exploring animal behavior through sound*. 2021, 1, 269-317.
6. Guex, A. G., Di Marzio, N., Eglin, D., Alini, M., & Serra, T. The waves that make the pattern: a review on acoustic manipulation in biomedical research. *Materials Today Bio*. 2021, 10, 100110.
7. Moges, K. A., Dalila, N., Plaskota, P., & Pyo, S. Evaluation Methods, Testing Standards, and Simulation Techniques of Sound Absorption Capabilities of Cementitious Materials: A Review. *Journal of Building Engineering*. 2024, 110468.
8. Indumathi Nallathambi, Padmaja Savaram, Sudhakar Sengan*, Meshal Alharbi, Samah Alshathri, Mohit Bajaj, Moustafa H. Aly and Walid El-Shafai, Impact of Fireworks Industry Safety Measures and Prevention Management System on Human Error Mitigation Using a Machine Learning Approach, *Sensors*, 2023, 23 (9), 4365; DOI:10.3390/s23094365.
9. Parkavi Krishnamoorthy, N. Sathesh, D. Sudha, Sudhakar Sengan, Meshal Alharbi, Denis A. Pustokhin, Irina V. Pustokhina, Roy Setiawan, Effective Scheduling of Multi-Load Automated Guided Vehicle in Spinning Mill: A Case Study, *IEEE Access*, 2023, DOI:10.1109/ACCESS.2023.3236843.
10. Ran Qian, Sudhakar Sengan, Sapna Juneja, English language teaching based on big data analytics in augmentative and alternative communication system, *Springer-International Journal of Speech Technology*, 2022, DOI:10.1007/s10772-022-09960-1.
11. Ngangbam Phalguni Singh, Shruti Suman, Thandaiah Prabu Ramachandran, Tripti Sharma, Selvakumar Raja, Rajasekar Rangasamy, Manikandan Parasuraman, Sudhakar Sengan, "Investigation on characteristics of Monte Carlo model of single electron transistor using Orthodox Theory", Elsevier, *Sustainable Energy Technologies and Assessments*, Vol. 48, 2021, 101601, DOI:10.1016/j.seta.2021.101601.
12. Huidan Huang, Xiaosu Wang, Sudhakar Sengan, Thota Chandu, Emotional intelligence for board capital on technological innovation performance of high-tech enterprises, Elsevier, *Aggression and Violent Behavior*, 2021, 101633, DOI:10.1016/j.avb.2021.101633.
13. Sudhakar Sengan, Kailash Kumar, V. Subramaniaswamy, Logesh Ravi, Cost-effective and efficient 3D human model creation and re-identification application for human digital twins, *Multimedia Tools and Applications*, DOI:10.1007/s11042-021-10842-y.
14. Prabhakaran Narayanan, Sudhakar Sengan*, Balasubramaniam Pudhupalayam Marimuthu, Ranjith Kumar Paulra, Novel Collision Detection and Avoidance System for Mid-vehicle Using Offset-Based Curvilinear Motion. *Wireless Personal Communication* 2021, 2021. DOI:10.1007/s11277-021-08333-2.
15. Balajee Alphonse, Venkatesan Rajagopal, Sudhakar Sengan, Kousalya Kittusamy, Amudha Kandasamy, Rajendiran Periyasamy Modeling and multi-class classification of vibroarthrographic signals via time domain curvilinear divergence random forest, *J Ambient Intell Human Comput*, 2021, DOI:10.1007/s12652-020-02869-0.

16. Omnia Saidani Neffati, Roy Setiawan, P Jayanthi, S Vanithamani, D K Sharma, R Regin, Devi Mani, Sudhakar Sengan*, An educational tool for enhanced mobile e-Learning for technical higher education using mobile devices for augmented reality, *Microprocessors and Microsystems*, Vol. 83, 2021, 104030, DOI:10.1016/j.micpro.2021.104030 .
17. Firas Tayseer Ayasrah, Nabeel S. Alsharafa, Sivaprakash S, Srinivasarao B, Sudhakar Sengan and Kumaran N, “Strategizing Low-Carbon Urban Planning through Environmental Impact Assessment by Artificial Intelligence-Driven Carbon Foot Print Forecasting”, *Journal of Machine and Computing*, Vol. 4, No. 04, 2024, doi: 10.53759/7669/jmc202404105.
18. Shaymaa Hussein Nowfal, Vijaya Bhaskar Sadu, Sudhakar Sengan*, Rajeshkumar G, Anjaneyulu Naik R, Sreekanth K, Genetic Algorithms for Optimized Selection of Biodegradable Polymers in Sustainable Manufacturing Processes, *Journal of Machine and Computing*, Vol. 4, No. 3, PP. 563-574, <https://doi.org/10.53759/7669/jmc202404054>.
19. Hayder M. A. Ghanimi, Sudhakar Sengan*, Vijaya Bhaskar Sadu, Parvinder Kaur, Manju Kaushik, Roobaea Alroobaea, Abdullah M. Baqasah, Majed Alsafyani & Pankaj Dadheech, An open-source MP + CNN + BiLSTM model-based hybrid model for recognizing sign language on smartphones. *Int J Syst Assur Eng Manag* (2024). <https://doi.org/10.1007/s13198-024-02376-x>
20. K. Bhavana Raj, Julian L. Webber, Divyapushpalakshmi Marimuthu, Abolfazl Mehbodniya, D. Stalin David, Rajasekar Rangasamy, Sudhakar Sengan, Equipment Planning for an Automated Production Line Using a Cloud System, *Innovations in Computer Science and Engineering. ICICSE Lecture Notes in Networks and Systems*, vol 565, pp 707–717, Springer, Singapore. DOI:10.1007/978-981-19-7455-7_57.
21. Zhang 2022, C., Li, H., Gong, J., Chen, J., Li, Z., Li, Q., ... & Zhang, J. (2023). The review of fiber-based sound-absorbing structures. *Textile Research Journal*, 93(1-2), 434-449.
22. Zhu, S., Cheng, D., & Tang, X. (2024). Recent advances on the fabrication and application of sound absorption coating-based textile composites. *Textile Research Journal*, 00405175241231827.
23. Gonçalves, F. S. S. R. (2022). Acoustic ecology in artistic creation: re-discovering underwater soundscapes (Doctoral dissertation, Universidade do Porto (Portugal)).
24. Wang, X., Xu, S., Bai, Y., Luo, X., Yang, M., & Huang, Z. (2024). Meta-barriers for ventilated sound reduction via transformation acoustics. *International Journal of Mechanical Sciences*, 274, 109262.
25. Shao, C., Xiong, W., Long, H., Tao, J., Cheng, Y., & Liu, X. (2021). Ultra-sparse metamaterials absorber for broadband low-frequency sound with free ventilation. *The Journal of the Acoustical Society of America*, 150(2), 1044-1056.
26. Ruan, H., & Li, D. Band gap characteristics of bionic acoustic metamaterials based on spider web: *engineering Structures*. 2024, 308, 118003.
27. Aydın, G., & San, S. E. Breaking the limits of acoustic science: A review of acoustic metamaterials. *Materials Science and Engineering: B*. 2024, 305, 117384.
28. Qin, X., Yang, W., Zhang, Z., & Chen, Z. Research on the design and noise reduction performance of periodic noise barriers based on nested structure. *Journal of Cleaner Production*. 2024, 143708.
29. Xiang, L., Wang, G., Zhu, C., Shi, M., Hu, J., & Luo, G. Ventilation barrier with space-coiling channels of varying cross-sections for broadband sound insulation. *Applied Acoustics*. 2022, 201, 109110.
30. Nakayama, M. Acoustic metamaterials based on polymer sheets: from material design to applications as sound insulators and vibration dampers. *Polym J* 56, 71–77 (2024). <https://doi.org/10.1038/s41428-023-00842-0>